Preprints of the 19th World Congress
The International Federation of Automatic Control
Cape Town, South Africa. August 24-29, 2014

Event-Triggered Control for Linear Systems Subject to Actuator Saturation

Wei Wu * **Sven Reimann** * **Steven Liu** *

* *Institute of Control Systems, University of Kaiserslautern*
P.O. Box 3049, 67653 Kaiserslautern, Germany
(e-mail: wu@eit.uni-kl.de, reimann@eit.uni-kl.de, sliu@eit.uni-kl.de).

Abstract: Event-triggered control is developed to reduce the communication load in networked control systems. This means that output or actuator signals are only transmitted over the network when an event-triggering condition is violated which is designed such that a certain control performance can be guaranteed. This paper considers event-triggered control subject to actuator saturation for linear systems. Therefore we present a method to estimate the domain of attraction which represents a contractive invariant set. The contractive invariant set is estimated by an ellipsoid which is determined by solving a linear matrix inequality (LMI) optimization problem. Further a controller synthesis design considering the event-triggering condition in our criterion is given to maximize the contractive ellipsoid. Simulations are given to illustrate the results.

Keywords: Event-triggered control; Linear matrix inequalities (LMIs); Actuator Saturation; Stability analysis; Optimization problems

1. INTRODUCTION

Event-triggered control has attracted much focus in recent years due to the promising advantage of less resource utilization compared to traditional periodic control, see Åström and Wittenmark [1990], Åström [2008], Årzn [1999], Lunze and Lehmann [2010], Wang and Lemmon [2011], Heemels et al. [2013], Tabuada [2007], Cogill [2009], Antunes et al. [2012]. The basic idea of event-triggered control is that when a certain control performance is still satisfactory then the execution of control tasks can be skipped and the transmission of the measured outputs or actuator signals can be saved. The saving of the resource is especially important for battery-powered wireless devices or for bandwidth-limited communication networks. Periodic event-triggered control is introduced by Heemels et al. [2013], where the plant states only need to be measured periodically. The measured data is processed by the so-called event generator to determine whether the actual control input is updated. The periodic event-triggered control strategy fits well the practical implementations for the standard time-sliced embedded software architectures.

One of the fundamental challenges for the design of event-triggered control systems lies in the design of approaches that can offer satisfactory control performance while reducing the control task executions and the data transmissions. In Lunze and Lehmann [2010] the performance of the event-based control system is evaluated by comparing this loop with the continuous-time state-feedback loop. The event generator utilizes a fixed threshold parameter. In Tabuada [2007], Anta and Tabuada [2010], Heemels et al. [2013], Wang and Lemmon [2011] the event-triggering conditions are designed to guarantee a certain decay rate of the Lyapunov function. In Eqtami et al. [2010], Li and Xu [2011] input-to-state stability is considered as the control performance based on which the event-triggering condition is determined. In Li and Xu [2011] additionally the controller is co-designed simultaneously with the event-triggering condition. In an optimal control framework the design of transmission sequences is studied in Cogill [2009], Antunes et al. [2012] for stochastic systems. The transmissions of actuator signals are included in the optimization process.

Basically in all practical systems the control input is constrained. This nonlinear characteristic demands further stability analysis. Concerning actuators subject to input saturation the stability and performance analysis are investigated in Lehmann et al. [2012], Kiener et al. [2012], Seuret et al. [2013]. In Lehmann et al. [2012], Kiener et al. [2012] the stability region under a constant threshold based event-triggered PI control is studied. In Seuret et al. [2013] a local exponentially stability is guaranteed by a designed event-triggering condition concerning an LQ cost function.

This paper first presents a criterion to analyse if a given ellipsoid is contractively invariant under an event-triggering condition. Then by introducing an auxiliary feedback matrix a novel event-triggering condition and controller co-design approach is presented aiming to maximize the contractive invariant set, see also Hu et al. [2002]. The control design approach generates a unique control gain after solving an LMI optimization problem. The simulation results show that the selected design parameter of the event-triggering condition has large influence on the size of the contractive invariant ellipsoid.

The remainder of the paper is organized into four sections. Section 2 introduces the linear system model and the necessary definitions and lemmas. In Section 3 the main approaches are given meanwhile the simulations for the derived results are accompanied. In Section 4 a conclusion is made.

Throughout the paper, the following notation is used: diag(·) denotes a block-diagonal matrix and tr(·) denotes the trace of a matrix. $\|\boldsymbol{x}\|$ denotes the Euclidean norm and $\|\boldsymbol{x}\|_\infty$:=max$_i$ $|x_i|$ denotes the infinity norm of a vector $\boldsymbol{x}$. Furthermore, a matrix $\begin{pmatrix} \boldsymbol{A} & * \\ \boldsymbol{B} & \boldsymbol{C} \end{pmatrix}$ represents a symmetric matrix $\begin{pmatrix} \boldsymbol{A} & \boldsymbol{B}^T \\ \boldsymbol{B} & \boldsymbol{C} \end{pmatrix}$.

2. PROBLEM FORMULATION

In this paper the considered plant is described by the continuous-time state equation subject to actuator saturation

$$\dot{\boldsymbol{x}}(t) = \boldsymbol{A}\boldsymbol{x}(t) + \boldsymbol{B}\text{sat}(\boldsymbol{u}(t)) \tag{1}$$

where $\boldsymbol{x}(t) \in \mathbb{R}^n$ is the state vector, $\boldsymbol{A} \in \mathbb{R}^{n\times n}$ is the system matrix, $\boldsymbol{B} \in \mathbb{R}^{n\times m}$ is the input matrix, and $\boldsymbol{u}(t) \in \mathbb{R}^m$ is the control signal. sat(·) is the standard saturation function, sat: $\mathbb{R}^m \to \mathbb{R}^m$ and $\text{sat}(\boldsymbol{u}) = (\text{sat}(u_1) \ \cdots \ \text{sat}(u_m))^T$, where $\text{sat}(u_j) = \text{sgn}(u_j)\min\{1, |u_j|\}$. The plant will be controlled in a periodic event-triggered way as in Heemels et al. [2013]. The measurement is made periodically with the time interval h at the time instances $t_k, k \in \mathbb{N}_0$ with $h = t_{k+1} - t_k$. The control input is updated using zero-order-hold (ZOH).

Remark 2.1. If the control input is not saturated by one but another value, i.e. $\text{sat}^*(u_j) = \text{sgn}(u_j)\min\{u_{j\max}, |u_j|\}$, the model can be transformed to the form of (1) with an input saturation of one for all inputs. Assume the model is given by

$$\dot{\boldsymbol{x}}(t) = \boldsymbol{A}\boldsymbol{x}(t) + \boldsymbol{B}^*\text{sat}^*(\boldsymbol{u}(t)) \tag{2}$$

with $\text{sat}^*(\boldsymbol{u}) = (\text{sat}^*(u_1) \ \cdots \ \text{sat}^*(u_m))^T$ which is equivalent to

$$\dot{\boldsymbol{x}}(t) = \boldsymbol{A}\boldsymbol{x}(t) + \boldsymbol{b}_1^*\text{sat}^*(u_1) + ... + \boldsymbol{b}_m^*\text{sat}^*(u_m) \tag{3}$$

where $\boldsymbol{B}^* = (\boldsymbol{b}_1^* \ \cdots \ \boldsymbol{b}_m^*)$. The model (3) can also be written as

$$\dot{\boldsymbol{x}}(t) = \boldsymbol{A}\boldsymbol{x}(t) + \sum_{j=1}^{m} \left(\boldsymbol{b}_j^* u_{j\max}\right) \frac{\text{sat}^*(u_j)}{u_{j\max}}. \tag{4}$$

Obviously $\frac{\text{sat}^*(u_j)}{u_{j\max}}$ is saturated by one, i.e. $\text{sat}(u_j) = \frac{\text{sat}^*(u_j)}{u_{j\max}}$. Therefore, the model (1) and (2) are equivalent by defining $\boldsymbol{B} = (\boldsymbol{b}_1 \ \cdots \ \boldsymbol{b}_m)$ with $\boldsymbol{b}_j = \boldsymbol{b}_j^* u_{i\max}$ for all $j = \{1, ..., m\}$. Consequently, any linear plant (2) with arbitrary saturation bounds can be transformed into a model (1) with saturation bounds equal one.

We are interested in obtaining the estimate of the domain of attraction of the system (1) under periodic event-triggered control. To maximize the domain of attraction an event-generator and controller synthesis is investigated. We first discretize the model (1) using ZOH to a sampled-data system model with respect to the measurement interval h, yielding

$$\boldsymbol{x}(k+1) = \boldsymbol{\Phi}\boldsymbol{x}(k) + \boldsymbol{\Gamma}\text{sat}\left(\boldsymbol{u}(k)\right) \tag{5}$$

with

$$\boldsymbol{\Phi} = e^{\boldsymbol{A}h}, \qquad \boldsymbol{\Gamma} = \int_0^h e^{\boldsymbol{A}s} ds \boldsymbol{B}$$

where $\boldsymbol{x}(k)$ is the measured state vector at the time instant t_k. In this paper a full state-feedback control law is considered

$$\boldsymbol{u}(k) = \boldsymbol{K}\hat{\boldsymbol{x}}^+(k), \tag{6}$$

where $\hat{\boldsymbol{x}}^+(k)$ is a signal defined in the time interval $(t_k, t_{k+1}]$ with

$$\hat{\boldsymbol{x}}^+(k) = \begin{cases} \boldsymbol{x}(k) & \text{if } \boldsymbol{u}(k) \text{ is updated} \\ \hat{\boldsymbol{x}}^+(k-1) & \text{if } \boldsymbol{u}(k) \text{ is not updated.} \end{cases} \tag{7}$$

and $\hat{\boldsymbol{x}}^+(k) = \boldsymbol{0}$ for $k \le 0$ with the initial time $k_0 = 0$. The decision for control updates is made by the event generator which is

$$\|\hat{\boldsymbol{x}}^+(k-1) - \boldsymbol{x}(k)\| > \sigma\|\boldsymbol{x}(k)\| \tag{8}$$

where $\sigma \in \mathbb{R}^+$, i.e. the control input $\boldsymbol{u}(k)$ is updated if condition (8) holds. This event-triggering condition is an important class of event-triggering conditions already applied in Heemels et al. [2013], Tabuada [2007], Wang and Lemmon [2011]. The state error based condition is motivated from the fact that the previous control input can be also effective if the states of the systems only have a minor change. Based on the event-triggering condition (8), (7) can be rewritten as

$$\hat{\boldsymbol{x}}^+(k) = \begin{cases} \boldsymbol{x}(k) & \text{if } \|\hat{\boldsymbol{x}}^+(k-1) - \boldsymbol{x}(k)\| > \sigma\|\boldsymbol{x}(k)\| \\ \hat{\boldsymbol{x}}^+(k-1) & \text{if } \|\hat{\boldsymbol{x}}^+(k-1) - \boldsymbol{x}(k)\| \le \sigma\|\boldsymbol{x}(k)\| \end{cases} \tag{9}$$

To investigate the attraction domain of system (5) the following definitions and Lemmas are introduced.

Notation 2.1. Given a matrix $\boldsymbol{H} \in \mathbb{R}^{m\times n}$, denote the j-th row of $\boldsymbol{H}$ as $\boldsymbol{h}_j$ and a symmetric polyhedron is defined

$$\mathcal{L}(\boldsymbol{H}) := \left\{\boldsymbol{x} \in \mathbb{R}^n : |\boldsymbol{h}_j\boldsymbol{x}| \le 1, j \in \mathbb{J} = \{1, ..., m\}\right\}. \tag{10}$$

Notation 2.2. Given a symmetric and positive definite matrix $\boldsymbol{P}$ and a positive scalar ρ, $\mathcal{E}(\boldsymbol{P}, \rho)$ represents the following ellipsoid

$$\mathcal{E}(\boldsymbol{P}, \rho) = \left\{\boldsymbol{x} \in \mathbb{R}^n : \boldsymbol{x}^T\boldsymbol{P}\boldsymbol{x} \le \rho\right\}. \tag{11}$$

Definition 2.1. A set $\mathcal{M}$ is said to be an invariant set with respect to a dynamic system if all the trajectories starting from it will remain in it, i.e.

$$\boldsymbol{x}(0) \in \mathcal{M} \ \Rightarrow \ \boldsymbol{x}(k) \in \mathcal{M} \ \ \forall k > 0.$$

Definition 2.2. Given a Lyapunov function

$$V(k) = \boldsymbol{x}^T(k)\boldsymbol{P}\boldsymbol{x}(k)$$

with $\boldsymbol{P}$ symmetric and positive definite the set $\mathcal{E}(\boldsymbol{P}, \rho)$ is called to be contractively invariant with respect to a dynamic system if

$$\Delta V(k) = \boldsymbol{x}^T(k+1)\boldsymbol{P}\boldsymbol{x}(k+1) - \boldsymbol{x}^T(k)\boldsymbol{P}\boldsymbol{x}(k) < 0 \tag{12}$$

for all $\boldsymbol{x} \in \mathcal{E}(\boldsymbol{P}, \rho)\backslash\{0\}$, i.e. the trajectories starting in the set $\mathcal{E}(\boldsymbol{P}, \rho)$ converge to the origin.

Notation 2.3. Let $\mathcal{D}$ be the set of all combinations of $m\times m$ diagonal matrices whose diagonal elements are either 1 or 0. Then there are 2^m elements in $\mathcal{D}$. Denote each element of $\mathcal{D}$ as $\boldsymbol{D}_i, i = 1, 2, ..., 2^m$. Then $\mathcal{D} = \left\{\boldsymbol{D}_i : i \in \{1, ..., 2^m\}\right\}$. Denote $\boldsymbol{D}_i^- = \boldsymbol{I} - \boldsymbol{D}_i$ and define the set $\mathbb{I} = \{1, ..., 2^m\}$.

Lemma 2.1. Hu et al. [2002] Let $\boldsymbol{u}$, $\boldsymbol{\nu} \in \mathbb{R}^m$. Suppose $\|\boldsymbol{\nu}\|_\infty \le 1$. Then

$$\text{sat}(\boldsymbol{u}) \in \text{co}\left\{\boldsymbol{D}_i\boldsymbol{u} + \boldsymbol{D}_i^-\boldsymbol{\nu} : i \in \mathbb{I}\right\},$$

where co{·} denotes the convex hull of a set.

Lemma 2.2. Given an ellipsoid $\mathcal{E}(\boldsymbol{P},\rho)$ and a polyhedron $\mathcal{L}(\boldsymbol{H})$, if

$$\begin{pmatrix} 1 & * \\ \boldsymbol{h}_j^T & \boldsymbol{P}/\rho \end{pmatrix} \geq 0, \quad j \in \mathbb{J}, \tag{13}$$

then $\mathcal{E}(\boldsymbol{P},\rho) \subset \mathcal{L}(\boldsymbol{H})$.

Proof. The proof can be found in [Boyd and Vandenberghe, 2004, pp. 414].

3. MAIN RESULT

Let's define the error variable

$$\boldsymbol{e}^+(k) = \hat{\boldsymbol{x}}^+(k) - \boldsymbol{x}(k) \tag{14}$$

in the time interval $(t_k, t_{k+1}]$. Based on the definition (9) the inequality

$$\|\boldsymbol{e}^+(k)\| \leq \sigma \|\boldsymbol{x}(k)\| \tag{15}$$

is always satisfied in the time interval $(t_k, t_{k+1}]$. With the control input $\boldsymbol{u}(k) = \boldsymbol{K}\hat{\boldsymbol{x}}^+(k)$ the closed-loop system of (5) is given by

$$\boldsymbol{x}(k+1) = \boldsymbol{\Phi}\boldsymbol{x}(k) + \boldsymbol{\Gamma}\mathrm{sat}\left(\boldsymbol{K}\hat{\boldsymbol{x}}^+(k)\right). \tag{16}$$

3.1 Contractive invariant set

In the first part of this section we propose a method for proving that a given ellipsoid is a contractively invariant set for a linear system with actuator saturation (5) which is controlled by the event-triggered control method (6),(9).

Theorem 3.1. Given an ellipsoid $\mathcal{E}(\boldsymbol{P},\rho)$, a control gain $\boldsymbol{K}$ and a positive scalar σ, if there exist a matrix $\boldsymbol{H} \in \mathbb{R}^{m\times n}$ and a scalar $\kappa > 0$ such that

$$\begin{pmatrix} \boldsymbol{P} - \hat{\boldsymbol{\Phi}}_i^T \boldsymbol{P} \hat{\boldsymbol{\Phi}}_i - \kappa\sigma^2 \boldsymbol{I} & * \\ -\boldsymbol{\Theta}_i^T \boldsymbol{\Gamma}^T \boldsymbol{P} \hat{\boldsymbol{\Phi}}_i & \kappa \boldsymbol{I} - \boldsymbol{\Theta}_i^T \boldsymbol{\Gamma}^T \boldsymbol{P} \boldsymbol{\Gamma} \boldsymbol{\Theta}_i \end{pmatrix} > 0 \tag{17}$$

for all $i \in \mathbb{I}$ with $\hat{\boldsymbol{\Phi}}_i = \boldsymbol{\Phi} + \boldsymbol{\Gamma}(\boldsymbol{D}_i\boldsymbol{K} + \boldsymbol{D}_i^-\boldsymbol{H})$, $\boldsymbol{\Theta}_i = \boldsymbol{D}_i\boldsymbol{K} + \boldsymbol{D}_i^-\boldsymbol{H}$ and $\mathcal{E}(\boldsymbol{P},\rho) \subset \mathcal{L}(\boldsymbol{H})$ i.e.

$$\begin{pmatrix} 1 & * \\ \boldsymbol{h}_j^T & \boldsymbol{P}/\rho \end{pmatrix} \geq 0 \quad \forall j \in \mathbb{J}, \tag{18}$$

then $\mathcal{E}(\boldsymbol{P},\rho)$ is a contractively invariant set for the closed-loop system (16).

Proof. For a given ellipsoid $\mathcal{E}(\boldsymbol{P},\rho)$, a corresponding quadratic Lyapunov function can be constructed by

$$V(k) = \boldsymbol{x}^T(k)\boldsymbol{P}\boldsymbol{x}(k). \tag{19}$$

Assume that the difference of the Lyapunov function $\Delta V(k) = V(k+1) - V(k)$ along the trajectories of the closed-loop system (16) satisfies

$$\boldsymbol{x}^T(k+1)\boldsymbol{P}\boldsymbol{x}(k+1) - \boldsymbol{x}^T(k)\boldsymbol{P}\boldsymbol{x}(k) < 0. \tag{20}$$

Substituting (16) in (20) results in

$$\begin{aligned} &\left(\boldsymbol{\Phi}\boldsymbol{x}(k) + \boldsymbol{\Gamma}\mathrm{sat}\left(\boldsymbol{K}\hat{\boldsymbol{x}}^+(k)\right)\right)^T \boldsymbol{P}\left(\boldsymbol{\Phi}\boldsymbol{x}(k) + \boldsymbol{\Gamma}\mathrm{sat}\left(\boldsymbol{K}\hat{\boldsymbol{x}}^+(k)\right)\right) \\ &- \boldsymbol{x}^T(k)\boldsymbol{P}\boldsymbol{x}(k) < 0, \end{aligned} \tag{21}$$

$\forall \boldsymbol{x}(k) \in \mathcal{E}(\boldsymbol{P},\rho) \setminus \{0\}$. According to the constraint $\mathcal{E}(\boldsymbol{P},\rho) \subset \mathcal{L}(\boldsymbol{H})$ it yields

$$|\boldsymbol{h}_j\boldsymbol{x}(k)| \leq 1, \quad \forall \boldsymbol{x}(k) \in \mathcal{E}(\boldsymbol{P},\rho), \quad j \in \mathbb{J}. \tag{22}$$

The definition of the variable $\hat{\boldsymbol{x}}^+(k)$ in (7) yields

$$\hat{\boldsymbol{x}}^+(k) \in \mathcal{E}(\boldsymbol{P},\rho), \quad \forall \boldsymbol{x}(k) \in \mathcal{E}(\boldsymbol{P},\rho).$$

Thus $\|\boldsymbol{H}\hat{\boldsymbol{x}}^+(k)\|_\infty \leq 1$. Based on Lemma 2.1

$$\mathrm{sat}\left(\boldsymbol{K}\hat{\boldsymbol{x}}^+(k)\right) \in \mathrm{co}\left\{\boldsymbol{D}_i\boldsymbol{K}\hat{\boldsymbol{x}}^+(k) + \boldsymbol{D}_i^-\boldsymbol{H}\hat{\boldsymbol{x}}^+(k) : i \in \mathbb{I}\right\}. \tag{23}$$

It follows that

$$\boldsymbol{\Phi}\boldsymbol{x}(k) + \boldsymbol{\Gamma}\mathrm{sat}\left(\boldsymbol{K}\hat{\boldsymbol{x}}^+(k)\right) \in \mathrm{co}\left\{\boldsymbol{\Phi}\boldsymbol{x}(k) + \boldsymbol{\Gamma}\boldsymbol{\Theta}_i\hat{\boldsymbol{x}}^+(k) : i \in \mathbb{I}\right\}. \tag{24}$$

with $\boldsymbol{\Theta}_i = (\boldsymbol{D}_i\boldsymbol{K} + \boldsymbol{D}_i^-\boldsymbol{H})$. The convexity of the quadratic function (19) gives

$$\begin{aligned} &\left(\boldsymbol{\Phi}\boldsymbol{x}(k) + \boldsymbol{\Gamma}\mathrm{sat}\left(\boldsymbol{K}\hat{\boldsymbol{x}}^+(k)\right)\right)^T \boldsymbol{P}\left(\boldsymbol{\Phi}\boldsymbol{x}(k) + \boldsymbol{\Gamma}\mathrm{sat}\left(\boldsymbol{K}\hat{\boldsymbol{x}}^+(k)\right)\right) \\ &\leq \max_{i\in\mathbb{I}} \left(\boldsymbol{\Phi}\boldsymbol{x}(k) + \boldsymbol{\Gamma}\boldsymbol{\Theta}_i\hat{\boldsymbol{x}}^+(k)\right)^T \boldsymbol{P}\left(\boldsymbol{\Phi}\boldsymbol{x}(k) + \boldsymbol{\Gamma}\boldsymbol{\Theta}_i\hat{\boldsymbol{x}}^+(k)\right). \end{aligned} \tag{25}$$

Therefore a sufficient condition satisfying (21) is

$$\begin{aligned} &\left(\boldsymbol{\Phi}\boldsymbol{x}(k) + \boldsymbol{\Theta}_i\hat{\boldsymbol{x}}^+(k)\right)^T \boldsymbol{P}\left(\boldsymbol{\Phi}\boldsymbol{x}(k) + \boldsymbol{\Theta}_i\hat{\boldsymbol{x}}^+(k)\right) \\ &- \boldsymbol{x}(k)^T\boldsymbol{P}\boldsymbol{x}(k) < 0, \quad \forall i \in \mathbb{I}. \end{aligned} \tag{26}$$

By substituting (14) into (26) we have

$$\boldsymbol{\Phi}\boldsymbol{x}(k) + \boldsymbol{\Gamma}\boldsymbol{\Theta}_i\hat{\boldsymbol{x}}^+(k) = \left(\boldsymbol{\Phi} + \boldsymbol{\Gamma}\boldsymbol{\Theta}_i\right)\boldsymbol{x}(k) + \boldsymbol{\Gamma}\boldsymbol{\Theta}_i\boldsymbol{e}^+(k). \tag{27}$$

Defining $\hat{\boldsymbol{\Phi}}_i = \boldsymbol{\Phi} + \boldsymbol{\Gamma}(\boldsymbol{D}_i\boldsymbol{K} + \boldsymbol{D}_i^-\boldsymbol{H})$ and substituting (27) into (26) yields

$$\begin{pmatrix} \boldsymbol{x}(k) \\ \boldsymbol{e}^+(k) \end{pmatrix}^T \hat{\boldsymbol{P}}_1 \begin{pmatrix} \boldsymbol{x}(k) \\ \boldsymbol{e}^+(k) \end{pmatrix} > 0 \tag{28}$$

with

$$\hat{\boldsymbol{P}}_1 = \begin{pmatrix} \boldsymbol{P} - \hat{\boldsymbol{\Phi}}_i^T \boldsymbol{P} \hat{\boldsymbol{\Phi}}_i & * \\ -\boldsymbol{\Theta}_i^T \boldsymbol{\Gamma}^T \boldsymbol{P} \hat{\boldsymbol{\Phi}}_i & -\boldsymbol{\Theta}_i^T \boldsymbol{\Gamma}^T \boldsymbol{P} \boldsymbol{\Gamma} \boldsymbol{\Theta}_i \end{pmatrix}. \tag{29}$$

The constraint (15) can be rewritten as

$$\begin{pmatrix} \boldsymbol{x}(k) \\ \boldsymbol{e}^+(k) \end{pmatrix}^T \begin{pmatrix} \sigma^2\boldsymbol{I} & \boldsymbol{0} \\ \boldsymbol{0} & -\boldsymbol{I} \end{pmatrix} \begin{pmatrix} \boldsymbol{x}(k) \\ \boldsymbol{e}^+(k) \end{pmatrix} \geq 0 \tag{30}$$

Applying the lossless S-procedure allows to combine the inequalities (28) and (30) to (17). The constraint $\mathcal{E}(\boldsymbol{P},\rho) \subset \mathcal{L}(\boldsymbol{H})$ can be expressed as the LMI (18) via Lemma 2.2. This completes the proof.

Theorem 3.1 can be extended to maximize the volume of the ellipsoid by maximizing the level value ρ for a given matrix $\boldsymbol{P}$.

Corollary 3.1. A maximization of the level value ρ is obtained for a given $\sigma > 0$ by the LMI optimization problem

$$\max \rho \text{ subject to (17) and (18)} \tag{31}$$

with the LMI variables $\boldsymbol{H} \in \mathbb{R}^{m\times n}$ and $\kappa \geq 0$.

Example 3.1. Considering the inverted pendulum as shown in Fig. 1 we investigate the relationship between σ in event-triggering condition (8) and the level value ρ of the ellipsoidal contractive invariant set. The linearized dynamic model of each inverted pendulum is given by

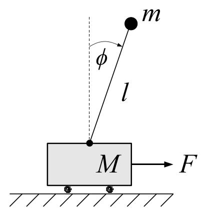

Fig. 1. An inverted pendulum

$$\begin{pmatrix}\dot\phi(t)\\ \ddot\phi(t)\end{pmatrix}=\begin{pmatrix}0 & 1\\ \frac{(m+M)g}{M\ell} & 0\end{pmatrix}\begin{pmatrix}\phi(t)\\ \dot\phi(t)\end{pmatrix}+\begin{pmatrix}0\\ \frac{-1}{M\ell}\end{pmatrix}\mathrm{sat}(u(t)).$$

where ϕ is the pendulum angle, u is the force acting on the cart with the pendulum mass $m = 0.1\,\mathrm{kg}$, the cart mass $M = 0.1\,\mathrm{kg}$, and the pendulum lengths $\ell = 0.136\,\mathrm{m}$. Gravitational acceleration is considered here equal to $g = 9.81\,\mathrm{m/s^2}$. The saturation bound is $u_{\max} = 1$ and the discretization interval is $h = 10\,\mathrm{ms}$ such that the sampled-data system is

$$\boldsymbol{x}(k+1)=\begin{pmatrix}1.0018 & 0.01\\ 0.36 & 1.0018\end{pmatrix}\boldsymbol{x}(k)+\begin{pmatrix}-0.001\\ -0.184\end{pmatrix}\mathrm{sat}(u(k)). \tag{32}$$

Further consider the given matrix

$$\boldsymbol{P}=\begin{pmatrix}68.341 & 2.785\\ 2.785 & 3.12\end{pmatrix},\quad \boldsymbol{K}=(5.394\ 5.024)\,.$$

The numerical results applying Corollary 3.1 are shown in Table 1 for a set of values of σ. In the last column we see the resulting update rate of a simulation lasting 10 seconds with an initial value $\boldsymbol{x}(0) = (0.2\ 0.8)^T$ for each case. The update rate is defined as ratio of number of events and number of samples in the simulation time.

σ	maximal ρ	$\boldsymbol{H}$	update rate
0.1	7.53	$(2.638\ 0.413)$	15.2 %
0.06	8.92	$(2.55\ 0.33)$	17.9 %
0.02	10.32	$(2.443\ 0.269)$	37.0 %

Table 1.

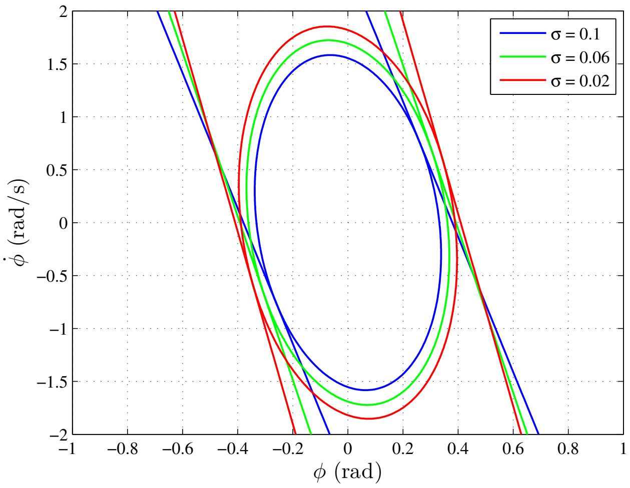

Fig. 2. Invariant ellipsoids determined with different σ in the event-triggering condition (15)

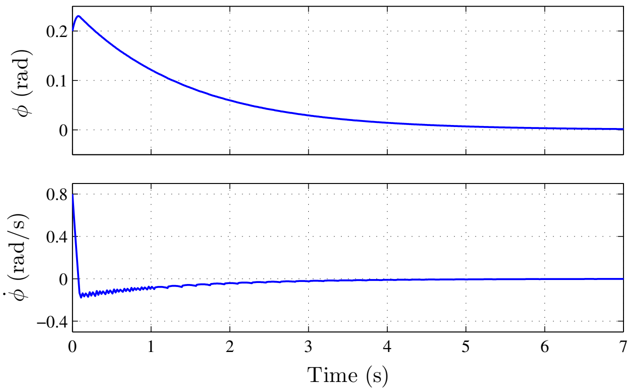

Fig. 3. Simulation results for $\sigma = 0.1$

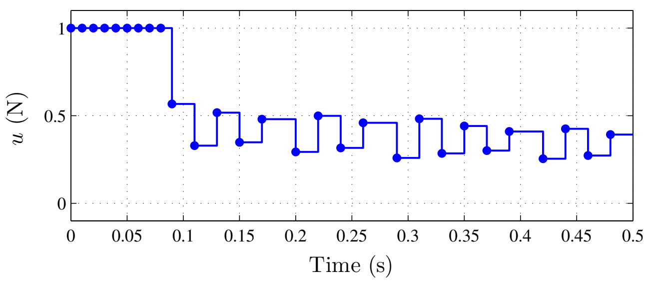

Fig. 4. Control input for the simulation with $\sigma = 0.1$ where a circles indicate the appearance of an event

The visualization of the invariant ellipsoids and polyhedrons is shown in Fig. 2 for the linear system (32). The nonlinear behaviour of the pendulum system for large angles is not taken into account as the approach only considers linear systems. The results show an inverse relationship between σ and ρ, i.e. increasing σ in the event-triggering condition (8) decreases the volume of the contractive invariant set of system (16). This also shows that the size of contractive invariant set and the update rate are correlated, i.e. for achieving a smaller update rate the size of the contractive invariant set is reduced. In applications a compromise between the size of the contractive invariant set and the update rate needs to be found.

In Fig. 3-4 the simulation results are shown for the event-triggered control approach with $\sigma = 0.1$. Fig. 3 shows the performance of the states and Fig. 4 shows the control input, the force on the cart in Newton. Especially in Fig. 4 we see that in the beginning the control input is saturated and at every time instant t_k an event occurs. From $t = 0.09\,\mathrm{s}$ the control input is not saturated anymore as the state vector approaches the origin and events only occur sparsely.

3.2 Controller synthesis

In Corollary 3.1 we proposed a method to maximize the level of a given contractive invariant set for a controlled linear system with the event-triggered mechanism. However an open problem is how to find the control matrix $\boldsymbol{K}$ and invariant set matrix $\boldsymbol{P}$. Therefore a controller synthesis is to be presented to design the invariant set jointly with the control matrix under the event-triggered control method. Thereby the aim is to maximize the size of the invariant ellipsoid for a given event-triggering parameter σ. One alternative to measure the geometrical size of the invariant ellipsoid is the volume, which is proportional to $(\det(\boldsymbol{P}^{-1}))^{1/2}$. The problem can be stated as

Problem 3.1. For the closed-loop system (16) find an event-triggered controller (6) such that for a given σ the volume of the invariant ellipsoid $\mathcal{E}(\boldsymbol{P}, 1)$ is maximized subject to condition (15) i.e.

$$\min_{\boldsymbol{K},\boldsymbol{P}} \text{logdet}\,(\boldsymbol{P}) \text{ subject to (16), (15) and} \tag{33}$$
$$\boldsymbol{x}^T(k+1)\boldsymbol{P}\boldsymbol{x}(k+1) - \boldsymbol{x}^T(k)\boldsymbol{P}\boldsymbol{x}(k) < 0 \;\; \forall \boldsymbol{x} \in \mathcal{E}(\boldsymbol{P},\rho)\backslash\{0\}.$$

Theorem 3.2. The solution to Problem 3.1 is obtained from the LMI optimization problem

$$\min_{\boldsymbol{P},\boldsymbol{K}} -\text{logdet}(\boldsymbol{S}) \quad \text{subject to} \tag{34a}$$
$$\begin{pmatrix} 1 & * \\ \boldsymbol{w}_j^T & \boldsymbol{G}^T + \boldsymbol{G} - \boldsymbol{S} \end{pmatrix} \geq 0, \tag{34b}$$
$$\begin{pmatrix} \boldsymbol{G}^T + \boldsymbol{G} - \boldsymbol{S} & * & * & * \\ \boldsymbol{0} & \boldsymbol{G}^T + \boldsymbol{G} - \kappa^{-1}\boldsymbol{I} & * & * \\ \boldsymbol{\Phi}\boldsymbol{G} + \boldsymbol{\Gamma}(\boldsymbol{\Theta_i}\boldsymbol{G}) & \boldsymbol{\Gamma}(\boldsymbol{\Theta_i}\boldsymbol{G}) & \boldsymbol{S} & * \\ \boldsymbol{G} & \boldsymbol{0} & \boldsymbol{0} & \frac{1}{\kappa\sigma^2}\boldsymbol{I} \end{pmatrix} > 0 \tag{34c}$$

for all $(i,j) \in \mathbb{I} \times \mathbb{J}$ with $\boldsymbol{\Theta_i G} = (\boldsymbol{D}_i\boldsymbol{K} + \boldsymbol{D}_i^-\boldsymbol{H})\boldsymbol{G} = (\boldsymbol{D}_i\boldsymbol{Y} + \boldsymbol{D}_i^-\boldsymbol{W})$ and the LMI variables $\boldsymbol{S} \in \mathbb{R}^{n\times n}$ symmetric and positive definite, $\boldsymbol{W} \in \mathbb{R}^{m\times n}$, $\boldsymbol{Y} \in \mathbb{R}^{m\times n}$ unrestricted, $\boldsymbol{w}_j$ being the j-th row of $\boldsymbol{W}$, $\boldsymbol{G} \in \mathbb{R}^{n\times n}$ invertible and $\kappa \geq 0$. The control gain and the Lyapunov matrix result from

$$\boldsymbol{K} = \boldsymbol{Y}\boldsymbol{G}^{-1}, \quad \boldsymbol{P} = \boldsymbol{S}^{-1}.$$

Proof. Consider a quadratic Lyapunov function

$$V(k) = \boldsymbol{x}^T(k)\boldsymbol{P}\boldsymbol{x}(k). \tag{35}$$

Following the same lines as the proof of Theorem 3.1 it can be shown based on the inequality

$$\begin{pmatrix} \boldsymbol{P} - \hat{\boldsymbol{\Phi}}_i^T\boldsymbol{P}\hat{\boldsymbol{\Phi}}_i - \kappa\sigma^2\boldsymbol{I} & * \\ -\boldsymbol{\Theta}_i^T\boldsymbol{\Gamma}^T\boldsymbol{P}\hat{\boldsymbol{\Phi}}_i & \kappa\boldsymbol{I} - \boldsymbol{\Theta}_i^T\boldsymbol{\Gamma}^T\boldsymbol{P}\boldsymbol{\Gamma}\boldsymbol{\Theta}_i \end{pmatrix} > 0 \tag{36}$$

that $\Delta V(k) = V(k+1) - V(k) < 0$ along the trajectories of the closed-loop system (16) for all $\boldsymbol{x}(k) \in \mathcal{L}(\boldsymbol{H})\backslash\{0\}$. Applying the Schur complement (36) is equivalent to

$$\begin{pmatrix} \boldsymbol{P} - \kappa\sigma^2\boldsymbol{I} & * & * \\ \boldsymbol{0} & \kappa\boldsymbol{I} & * \\ \hat{\boldsymbol{\Phi}}_i & \boldsymbol{\Gamma}\boldsymbol{\Theta}_i & \boldsymbol{P}^{-1} \end{pmatrix} > 0. \tag{37}$$

Using Schur-Complement again (37) is transformed to

$$\begin{pmatrix} \boldsymbol{P} & * & * & * \\ \boldsymbol{0} & \kappa\boldsymbol{I} & * & * \\ \hat{\boldsymbol{\Phi}}_i & \boldsymbol{\Gamma}\boldsymbol{\Theta}_i & \boldsymbol{P}^{-1} & * \\ \boldsymbol{I} & \boldsymbol{0} & \boldsymbol{0} & \frac{1}{\kappa\sigma^2}\boldsymbol{I} \end{pmatrix} > 0. \tag{38}$$

Pre-/post-multiplying (38) by $\text{diag}\big(\boldsymbol{G}^T, \boldsymbol{G}^T, \boldsymbol{I}, \boldsymbol{I}\big)$ and $\text{diag}\big(\boldsymbol{G}, \boldsymbol{G}, \boldsymbol{I}, \boldsymbol{I}\big)$ respectively yields

$$\begin{pmatrix} \boldsymbol{G}^T\boldsymbol{P}\boldsymbol{G} & * & * & * \\ \boldsymbol{0} & \kappa\boldsymbol{G}^T\boldsymbol{G} & * & * \\ \hat{\boldsymbol{\Phi}}_i\boldsymbol{G} & \boldsymbol{\Gamma}\boldsymbol{\Theta}_i\boldsymbol{G} & \boldsymbol{P}^{-1} & * \\ \boldsymbol{G} & \boldsymbol{0} & \boldsymbol{0} & \frac{1}{\kappa\sigma^2}\boldsymbol{I} \end{pmatrix} > 0. \tag{39}$$

Since the identity matrix $\boldsymbol{I}$ and $\boldsymbol{P}$ are symmetric and positive definite and $\kappa \geq 0$, also

$$\left(\kappa^{-1}\boldsymbol{I} - \boldsymbol{G}\right)^T \kappa\boldsymbol{I}\left(\kappa^{-1}\boldsymbol{I} - \boldsymbol{G}\right) \geq \boldsymbol{0} \tag{40}$$
$$\left(\boldsymbol{P}^{-1} - \boldsymbol{G}\right)^T \boldsymbol{P}\left(\boldsymbol{P}^{-1} - \boldsymbol{G}\right) \geq \boldsymbol{0} \tag{41}$$

hold as inversion and congruence transformation do not affect definiteness. The inequalities (40) and (41) are equivalent to

$$\kappa\boldsymbol{G}^T\boldsymbol{G} \geq \boldsymbol{G}^T + \boldsymbol{G} - \kappa^{-1}\boldsymbol{I} \tag{42}$$
$$\boldsymbol{G}^T\boldsymbol{P}\boldsymbol{G} \geq \boldsymbol{G}^T + \boldsymbol{G} - \boldsymbol{P}^{-1} \tag{43}$$

Therefore, a sufficient condition for (39) is

$$\begin{pmatrix} \boldsymbol{G}^T + \boldsymbol{G} - \boldsymbol{P}^{-1} & * & * & * \\ \boldsymbol{0} & \boldsymbol{G}^T + \boldsymbol{G} - \kappa^{-1}\boldsymbol{I} & * & * \\ \hat{\boldsymbol{\Phi}}_i\boldsymbol{G} & \boldsymbol{\Gamma}\boldsymbol{\Theta}_i\boldsymbol{G} & \boldsymbol{P}^{-1} & * \\ \boldsymbol{G} & \boldsymbol{0} & \boldsymbol{0} & \frac{1}{\kappa\sigma^2}\boldsymbol{I} \end{pmatrix} > 0. \tag{44}$$

Substituting $\boldsymbol{S} = \boldsymbol{P}^{-1}$, $\boldsymbol{K} = \boldsymbol{Y}\boldsymbol{G}^{-1}$ and $\boldsymbol{H} = \boldsymbol{W}\boldsymbol{G}^{-1}$ the inequalities (44) and (34c) are equivalent. Furthermore the constraint $\mathcal{E}(\boldsymbol{P}, 1) \subset \mathcal{L}(\boldsymbol{H})$ can be written as

$$\begin{pmatrix} 1 & * \\ \boldsymbol{h}_j^T & \boldsymbol{P} \end{pmatrix} \geq 0, \quad j \in \mathbb{J}. \tag{45}$$

Pre-/post-multiplying (45) $\text{diag}\big(\boldsymbol{I}, \boldsymbol{G}^T\big)$ and $\text{diag}\big(\boldsymbol{I}, \boldsymbol{G}\big)$ respectively yields

$$\begin{pmatrix} 1 & * \\ \boldsymbol{G}^T\boldsymbol{h}_j^T & \boldsymbol{G}^T\boldsymbol{P}\boldsymbol{G} \end{pmatrix} \geq 0, \quad j \in \mathbb{J}. \tag{46}$$

Using (43) and substituting $\boldsymbol{w}_j^T = \boldsymbol{G}^T\boldsymbol{h}_j^T$ it is shown that (34b) is a sufficient condition for (46).

For inspecting the objective function Problem 3.1 we substitute $\boldsymbol{P} = \boldsymbol{S}^{-1}$. Since $-\text{logdet}(\boldsymbol{S})$ is already defined in the MATLAB toolbox YALMIP Löfberg [2004] it can be solved directly using the SeDuMi solver Sturm [1999]. This completes the proof.

Example 3.2. Consider the second order inverted pendulum system (32) in Example 3.1 again. Table 2 gives the

σ	$\boldsymbol{K}$	$\boldsymbol{H}$	update rate
0.1	$\begin{pmatrix}6.3717 & 2.6619\end{pmatrix}$	$\begin{pmatrix}2.2412 & 0.4264\end{pmatrix}$	21.8 %
0.06	$\begin{pmatrix}8.9800 & 2.3006\end{pmatrix}$	$\begin{pmatrix}2.1490 & 0.3805\end{pmatrix}$	50.6 %
0.02	$\begin{pmatrix}11.2366 & 1.9868\end{pmatrix}$	$\begin{pmatrix}2.1132 & 0.3549\end{pmatrix}$	99.9 %

Table 2.

results from the application of Theorem 3.2 and from the simulation with the initial state $\boldsymbol{x}(0) = (0.2\ 0.8)^T$ and a simulation time of 10 seconds. Meanwhile Fig. 5 shows the corresponding contractive invariant ellipsoids. The obtained ellipsoids are always bigger than the ones from Example 3.1 with the random selected control gain and ellipsoidal estimate.

Fig. 6 shows the contractive invariant ellipsoids for $\sigma = 0.06$ from Corollary 3.1 with the ellipsoid and control gain parameters from Example 3.1 and Theorem 3.2 as well as the path under the initial state $\boldsymbol{x}(0) = (-0.6303\ 1.426)$ (red). The initial state is chosen inside the estimated ellipsoid derived from Theorem 3.2 but outside the one obtained from Corollary 3.1. The path under the random controller (dashed) is obviously diverging and the controller synthesis allows to realize a larger ellipsoid such that the path (solid) is converging to the origin, which shows the effectiveness of the proposed controller synthesis approach.

4. CONCLUSION

In this paper a novel event-triggering condition and controller synthesis approach is studied for the linear system subject to actuator saturation. By synthesizing the feedback control gain and the event-triggering conditions

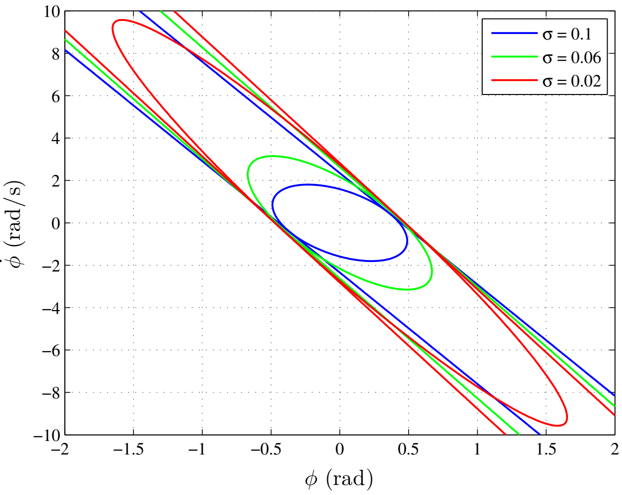

Fig. 5. Invariant ellipsoids determined by controller synthesis for different σ

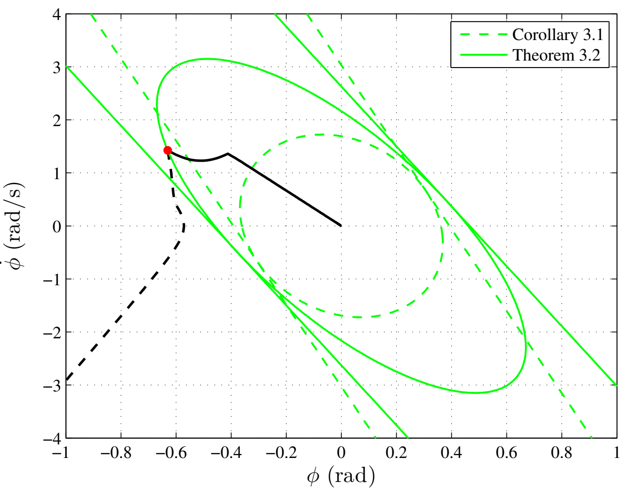

Fig. 6. Comparison of Corollary 3.1 (dashed) and Theorem 3.2 (solid)

in LMIs an optimization for obtaining the maximal contractive invariant set is achieved. The results can also easily be extended to cover the case with constant delay in the system model. Compared with the existing results in Lehmann et al. [2012], Kiener et al. [2012], Seuret et al. [2013] our results allow the controller design in an optimization problem by the presented criteria, which is a new contribution to the event-triggered control.

REFERENCES

A. Anta and P. Tabuada. On the minimum attention and anytime attention problems for nonlinear systems. In *Proceedings of the 49th IEEE Conference on Decision and Control*, pages 3234–3239, 2010.

D. Antunes, W. P. M. H. Heemels, and P. Tabuada. Dynamic programming formulation of periodic event-triggered control: Performance guarantees and co-design. In *Proceedings of the 51st IEEE Conference on Decision and Control*, pages 7212–7217, 2012.

Karl-Erik Årzn. A simple event-based PID controller. In *Proceedings 14th World Congress of IFAC*, pages 423–428, 1999.

K. J. Åström. Event based control. In Alessandro Astolfi and Lorenzo Marconi, editors, *Analysis and Design of Nonlinear Control Systems: In Honor of Alberto Isidori*, pages 127–147. Springer, Berlin, 2008.

K. J. Åström and B. Wittenmark. *Computer-Controlled Systems: Theory and Design*. Prentice-Hall, Englewood Cliffs, NJ, 2nd edition, 1990.

S. Boyd and L. Vandenberghe. *Convex Optimization.* Cambridge University press, 2004.

R. Cogill. Event-based control using quadratic approximate value functions. In *Proceedings of the 48th IEEE Conference on Decision and Control*, pages 5883–5888, 2009.

A. Eqtami, D. V. Dimarogonas, and K. J. Kyriakopoulos. Event-triggered control for discrete-time systems. In *Proceedings of the 2010 American Control Conference*, pages 4719–4724, 2010.

W. P. M. H. Heemels, M. C. F. Donkers, and A. R. Teel. Periodic event-triggered control for linear systems. *IEEE Transactions on Automatic Control*, 58(4):847–861, 2013.

T. Hu, Z. Lin, and B. M. Chen. Analysis and design for discrete-time linear systems subject to actuator saturation. *Systems & Control Letters*, 45:97–112, 2002.

G. A. Kiener, D. Lehmann, and K. H. Johansson. Actuator saturation and anti-windup compensation in event-triggered control. *Discrete Event Dynamic Systems: Theory and Applications*, 2012.

D. Lehmann, G. A. Kiener, and K. H. Johansson. Event-triggered pi control: Saturating actuator and anti-windup compensation. In *Proceedings of the 51st IEEE Conference on Decision and Control*, 2012.

S. B. Li and B. G. Xu. Co-design of event generator and controller for event-triggered control system. In *Proceedings of the Chinese Control Conference*, pages 175–179, 2011.

J. Löfberg. Yalmip : A toolbox for modeling and optimization in MATLAB. In *Proceedings of the 2004 IEEE International Symposium on Computer Aided Control Systems Design*, pages 284–289, 2004.

J. Lunze and D. Lehmann. A state-feedback approach to event-based control. *Automatica*, 46(1):211–215, 2010.

A. Seuret, C. Prieur, S. Tarbouriech, and L. Zaccarian. Event-triggered control with LQ optimality guarantees for saturated linear systems. In *9th IFAC Symposium on Nonlinear Control Systems*, 2013.

J. F. Sturm. Using SeDuMi 1.02, a MATLAB toolbox for optimization over symmetric cones (updated for version 1.3). *Optimization Methods and Software*, 11-12:625–653, 1999.

P. Tabuada. Event-triggered real-time scheduling of stabilizing control tasks. *IEEE Transactions on Automatic Control*, 52(4):1680–1685, 2007.

X. Wang and M. D. Lemmon. Event-triggering in distributed networked control systems. *IEEE Transactions on Automatic Control*, 56:586–601, 2011.